Title

A chronotype effect: circadian-period variation underlies the local adaptation of photoperiodism in the short-day plant *Lemna aequinoctialis.*

Authors

Tomoaki Muranaka[1], Shogo Ito[2], Hiroshi Kudoh[3], Tokitaka Oyama[2*]

1. Faculty of Agriculture, Kagoshima University, Korimoto 21-24-1, Kagoshima, 890-0065, Japan
2. Department of Botany, Graduate School of Science, Kyoto University, Kitashirakawa-Oiwake-cho, Sakyo-ku, Kyoto, 606-8502, Japan
3. Center for Ecological Research, Kyoto University, Hirano 2-509-3, Otsu, 520-2113, Japan

*Corresponding author (email): oyama.tokitaka.8w@kyoto-u.ac.jp

Summary

Phenotypic variation is the basis for trait adaptation via evolutionary selection.[1, 2, 3] However, the driving forces behind the quantitative trait variations in natural settings remain unclear owing to their complexity at the molecular level.[4, 5, 6] This study focused on the natural variation of the free-running period (FRP) of the circadian clock as FRP is a determining factor of the internal clock phase (chronotype), which is responsible for physiological timing during a day.[7] Although natural variations in FRP have been widely reported,[8, 9, 10, 11] few studies have shown the association between FRP and adaptive temporal traits. As a clock-dependent physiological process, photoperiodism is a typical target of local adaptation.[12, 13] *Lemna aequinoctialis* in Japan is a paddy-field duckweed exhibiting a latitudinal cline of critical day-lengths (CDLs) for short-day flowering.[14] To investigate the relationship between FRP and CDL, we collected 72 strains of *L. aequinoctialis* within a latitudinal range between 31.5°N to 43.8°N. We found a significant correlation (P = 7.5E-8) between FRPs and locally adaptive CDLs, confirming that the variation in FRP-dependent chronotypes underlies geographically differentiated photoperiodism. Diel transcriptome analysis revealed that the induction timing of a florigen gene is key for connecting chronotypes to photoperiodism at the molecular level. Based on these results, we propose a fundamental rule concerning the "chronotype effect" in evolution: the variation of circadian period functions as a resource for the variation of temporal traits. This study highlights the adaptive significance of circadian-period variation and provides a reason for the maintenance of period variation in natural populations.

Results and discussions.

We investigated the influence of natural variations in circadian clock properties on the temporal phenotype of clock-dependent physiology. The circadian clock is an endogenous timing system that generates a self-sustained daily oscillation entrained to day-night cycles via environmental cues.[15] The eukaryotic circadian clock consists of feedback loops of multiple clock genes.[16] The free-running period (FRP) of the circadian clock is a polygenic trait that exhibits natural variation.[8, 9, 10, 11, 12, 17] These circadian clocks with different periods are entrained to 24 h day-night cycles.[18, 19] The peak timing (phase) of an entrained rhythm also shows natural variation. This phase phenotype is termed the chronotype.[7] In this study, we define the "chronotype effect" as the phenotypic effects on physiological traits originating from variations in chronotype. Previous studies suggest that chronotype determination is related to the FRP.[20, 21, 22, 23, 24, 25, 26] We hypothesized that FRP variation is associated with local adaptation of a clock-dependent physiology.

Lemna aequinoctialis in Japan is a paddy-field duckweed with a latitudinal cline of critical day-lengths (CDLs) for short-day flowering.[14] To investigate the relationship between FRP and CDL, we collected 72 strains of *L. aequinoctialis* from 20 populations located between latitudes 31.5°N and 43.8°N (Fig. 1a and Table S1). To estimate both intra-population and inter-population variation, 11–12 strains were collected from each of four populations (N32Ka, N35Ht, N35So, and N44Ha). The strains were aseptically maintained by clonal growth. Laboratory experiments using a clonal plant enabled the precise determination of multiple phenotypic traits of the natural genotype. The frond size showed intra-population and inter-population variation, suggesting heterogeneous genotypes, even within a population (Fig. S1). The estimated genome sizes of all the strains were similar (Fig. S2).

These strains recognized day lengths with a resolution of 0.5 h and their CDLs ranged from 11.2 to 14.2 h (Fig. S3). As previously reported,[14] a latitudinal cline was observed in CDLs: 11.2–12.6 h in the south, 12.4–14.2 h in the north, and a large variation of CDLs was observed at approximately 35°N (Fig. 1b). The longer CDL at higher latitudes is consistent with other short-day flowering species.[27, 28, 29] Intra-population differences of 1–1.5 h in CDLs were observed in each population of N32Ka, N35Ht, N35So, and N44Ha (Fig. 1c). The significant differences between these populations suggest geographical differentiation of CDLs. The difference in CDL between the two 35°N populations, N35Ht and N35So suggests that the adaptive CDL at each site may differ even at the same latitude (Fig. 1c). The flooding period of the paddy fields differed between the sampling sites depending on the cultivation schedule of the different rice cultivars. The longer CDL of N35So, corresponding to earlier flowering, is consistent with the earlier cessation of flooding at this site than that at the N35Ht site (Fig. 1d). The CDL of the N32Ka population was shorter than that of the N35 population (Fig. 1c). The CDLs of the three populations appeared to be linked to the cultivation schedule at each site (Fig. 1d). Complete drainage of paddy fields during and after rice harvesting is a potential selection pressure for duckweed.[30, 31] Although the rice-harvesting time at the N44Ha site

was comparable to that at the N35Ht site, the CDL of N44Ha was longer than that of N35Ht. At the N44Ha site, the low-temperature season (<15 °C: lower limit for *L. aequinoctialis* growth)[32] began before the rice harvest time, suggesting that low temperature, rather than rice harvest time, may be a potential selection pressure. Overall, the CDLs of the four populations were likely to fit a suitable season for reproduction at each site.

The natural variation in circadian rhythms was assessed using a luciferase reporter assay.[33] Using particle bombardment, a luminescent reporter, *AtCCA1::LUC*,[34] was semi-transiently introduced into plants grown under long-day conditions (15L9D; 15-h light / 9-h dark). The plants were placed on an automatic luminescent monitoring system and released into constant light (LL) after two days of 15L9D (Fig. 2a). All strains showed clear diel luminescence rhythms with morning peaks at 15L9D. Among the four populations, the peak time of N32Ka was significantly later than that of the other three populations (Fig. 2b). To estimate FRP under LL, fast Fourier transform-nonlinear least squares (FFT-NLLS) analysis was used (Fig. 2c)[35], in which the rhythm significance was estimated by a relative amplitude error (RAE) that increased from 0 to 1 as the rhythm neared statistical insignificance. Seven strains with a high RAE value (>0.1) or a high standard deviation (SD) of FRP (>1.5 h) were excluded from the following analysis (Fig. S4). The FRP of N32Ka was significantly longer than that of the other populations, corresponding to its late peak time (Fig. 2b and d). This is consistent with the concept of chronotype: a positive correlation between FRP and peak time.[24]

Correlation analysis using data from all 72 strains (20 populations) suggested a chronotype effect on photoperiodism (Fig. 3a). A positive correlation between FRP and peak time was confirmed at the genotypic level. In addition, CDL showed a negative correlation with both FRP and the peak time. These results suggest that the variation in FRP-dependent chronotypes underlies the variation in the CDL. The CDL shift can be explained as the chronotype effect on the florigen (floral inducer), which responds to night-length (Fig. 3b).[36] In this model, the activation of the florigen is assumed to be gated by the circadian clock and permitted in the dark. A longer FRP causes a phase delay in the gate timing and, consequently, a shorter CDL, resulting in a negative correlation between FRP and CDL.[37]

To explore florigen genes, we obtained diel transcriptomes of *L. aequnictialis* pure line (Nd strain[33]) under three photoperiod conditions. Five florigen homologues were detected by *de novo* assembly and were named *LaFTh1–5* (Fig. S5). *LaFTh1* was induced before the end of the night, and its expression level increased during longer-night conditions (Fig. 3c). The transgenic *Arabidopsis thaliana* carrying an *LaFTh1* overexpression construct showed an early flowering phenotype, suggesting its florigen activity (Fig. S6). *LaFTh1* was induced even in extended dark following a non-flowering long-day condition, suggesting that *LaFTh1* expression directly responds to night lengthening. The timing of *LaFTh1* induction differed among the three strains with different CDLs and the variation in induction timing appears to be responsible for the CDL variation (Fig. 3d and e).

Thus, the induction timing of *LaFTh1* is key for connecting chronotype to photoperiodism at the molecular level. Notably, the *LaFTh1* expression levels showed a large difference. The *LaFTh1* expression in the N44Ha08 strain was 10-fold higher than that in the other two strains (Fig. 3e). This high basal level may have caused an extremely long CDL of 14.2 h (Fig. 1c).

Our study demonstrated the chronotype effect on locally adapted traits: CDL variation is tightly coupled with FRP variation, even in natural populations. Diel transcriptome analysis suggests that florigen induction timing, which is likely to be related to the FRP-dependent chronotype, is a determining factor for CDL and consequently for the flowering season. These results indicate the importance of circadian phenotypes in the natural selection of seasonal phenotypes. This study also provides new insights into the local adaptation of CDLs to the paddy-field environment. Consistent with previous studies using short-day plants,[27, 28, 29] the populations of *L. aequinctialis* in Japan showed a latitudinal cline in their CDLs, suggesting that the flowering season of this plant adapted to the local climate, exhibiting a latitudinal cline in temperature.[12] Furthermore, their CDLs appeared to adapt to the flooding season at each sampling site (Fig. 1d). The improved drainage systems associated with the agricultural modernization of Japan that began in the 1950s have resulted in dry paddy-field environments in winter and consequently altered the weed flora.[38] The natural variation of the FRPs possibly contributed to the adaptive evolution of the flowering season in response to the rapid artificial shift of the flooding season. In addition to inter-population variations, CDLs also showed intra-population variations (Fig. 1c). The flooding period of paddy fields is highly dependent on the rice cultivar grown. Such artificial fluctuations may promote intra-population variations in CDLs. In *A. thaliana*, the recombinant inbred lines of two accessions with similar FPRs showed variation as substantial as that observed among the global collection (22.0 to 28.5 h).[39] Such transgressive segregation of FPR is caused by the complex interference among many quantitative loci,[40] and may play an important role in providing the phenotypic variations for rapid evolutionary adaptation to irregular environmental changes.[41] Interestingly, the estimated genome sizes of all *L. aequinoctialis* strains used in this study were ~800 Mbp and considered to be tetraploid (Fig. S2).[42, 43] Polyploidy may generate phenotypic variations by increasing the rates of evolution and number of components in gene regulatory networks.[44, 45]

Because the circadian clock regulates various physiologies,[7, 46] FRP variation potentially contributes to the fine-tuning of their temporal traits in the process of local adaptation. Conversely, selection pressure on the temporal traits of such clock-dependent physiologies may favor mutations in clock-related genes that alter the FRP and, consequently, the chronotype (Fig. 4). This is a possible reason for the maintenance of FRP variation with standing genetic variations in clock-related genes in natural populations.[8, 11, 12] Thus, the adaptive significance of FRP variation should be considered in relation to the phase phenotype under day-night conditions.[7, 21, 25] Interestingly, a latitudinal cline of FRP was reported in the linden bug, *Pyrrhocoris apterus*,[10] in which circadian clock genes are

145 responsible for the photoperiodic response of the reproductive diapause.[47] The circadian clock was
146 acquired for adaptation to day-night cycles and has evolved as a hub of environmental response
147 systems involving multiple input pathways.[48] As a result, in the process of adaptive evolution, the
148 circadian system can function as a source of variation for temporal traits through the chronotype effect
149 integrating many quantitative loci for FRP.[4, 39, 49, 50]
150

Methods

Plant materials and growth conditions. Seventy-two *L. aequinoctialis* strains were collected from 20 sites in Japan (Table S1). The collected plants were sterilized by washing with 5% sodium hypochlorite for several minutes, followed by washing with sterilized water. From the successfully sterilized plants, a single colony was isolated. Only one strain was isolated from a paddy field, and a maximum of 12 paddy fields were selected at each site. These strains were maintained aseptically in a growth medium (NF medium containing 1% sucrose[33]) under long-day conditions (15L9D; approximately 50 μmol m^{-2} s^{-1}) in an incubator (LH350-SP, NK system, Japan) at 25 ± 1 °C. Before the experiments, the plants were grown in a flask or 6-well plastic plate filled with 30 mL or 8 mL of growth medium, respectively.

Genome size estimation. The relative genome sizes of *L. aequinoctialis* strains were estimated based on 4',6-diamidino-2-phenylindole diacetate dye flow cytometry (DAPI-FCM) using a Partec CyStain UV Precise P reagent kit (Sysmex Partec GmbH, Germany) and a flow cytometer (Partec Ploidy Analyzer PA-I, Sysmex Partec GmbH). *Lemna gibba* p8L[33] was used as the standard. The relative genome sizes of th*e L. aequinoctialis* strains were calculated as the relative peak positions. The genome size of *L. gibba* has been estimated to be 486 Mbp.[43]

Frond-length measurements. The top view image of the plants was captured using a digital camera (EOS 5D mark3 [Canon, Japan] with SP 90 mm Di MACRO [Tamron, Japan] or EOS Kiss X5 with EF-S55-250 mm [Canon]). The frond length was manually measured as the length from the base to the apex of the mother frond using ImageJ 1.53c software (Fig. S1a).[51] The frond lengths of the eight colonies were measured for each strain.

Measurement of the critical day length in photoperiodic flowering. A colony consisting of three or four visible fronds was placed in each well of a 24-well plastic plate filled with 2 mL of growth medium. These plants were subjected to a one-week photoperiodic treatment with day lengths of 9, 11, 11.5, 12, 12.5, 13, 13.5, 14, 14.5, and 15 h in an eight-chamber incubator (LH30-8-CT, NK system, Japan). The temperature was maintained at 25 ± 1 °C and the light intensity was approximately 30 μmol m^{-2} s^{-1}. After treatment, the plants were bleached with 70% ethanol. The number of flowering and non-flowering fronds was counted for each colony under a stereoscopic microscope. Flowering rate was calculated as the percentage of flowering fronds to the total number of fronds in at least two replicates. The critical day length was determined as the day length where 50% of the maximum flowering rate (Fmax) was expected in a piecewise linear function for the obtained flowering rate (Fig. S3c).

187 **Meteorological data**
188 Temperature data at each site were obtained from the Automated Meteorological Data Acquisition
189 System (AMeDAS) data download service (https://www.data.jma.go.jp/risk/obsdl/index.php). Day
190 lengths were calculated using the online service of the National Astronomical Observatory of Japan
191 (https://eco.mtk.nao.ac.jp/cgi-bin/koyomi/koyomix_en.cgi).
192
193 **Monitoring luminescence rhythms.** Luminescence monitoring using a circadian luminescent
194 reporter was performed as previously described[33]. Plasmid DNA carrying the luciferase reporter gene
195 *pUC-AtCCA1::LUC+* (*AtCCA1::LUC*[34]) was coated on 0.48 mg of gold particles (1.0 μm diameter,
196 Bio-Rad) and introduced into plants laid on a 60-mm plastic dish using a particle bombardment system
197 (PDS-1000/He, Bio-Rad) according to the manufacturer's instructions (vacuum, 27 mmHg; helium
198 pressure, 450 psi). After particle bombardment, the plants were divided into three 35-mm dishes
199 (approximately four colonies per dish) filled with 4 mL of growth medium containing D-luciferin (0.2
200 mM potassium salt, Wako). A luminescence dish-monitoring system with photomultiplier tubes
201 (H7360-01; Hamamatsu Photonics K.K., Japan) was used for the luminescence measurements. To
202 reduce the background chlorophyll fluorescence, a short-pass filter (SVO630; Asahi Spectra, Japan)
203 was set at the detection site of the photomultiplier tubes. Each dish was subjected to 30 s of
204 measurements every 20 min. The monitoring system was placed in an incubator (KCLP-1000I-CT;
205 NK System, Japan) with fluorescent lamps (FL20SSW/18; Mitsubishi Electric Co., Japan). The
206 temperature was maintained at 25 ± 1 °C and the light intensity was approximately 30 μmol m^{-2} s^{-1}.
207
208 **Time-series analysis.** Peak detection and period estimation were performed as previously described.[33,
209 52] The peak positions were estimated by local quadratic curve fitting. For period estimation, the
210 obtained luminescence time series were detrended by subtracting the 24-h moving average. Thereafter,
211 the amplitude was normalized by dividing by the 24-h moving standard deviation. The normalized
212 time series of 60 to 132 h was analyzed using fast Fourier transform-nonlinear least squares (FFT-
213 NLLS) to determine the period.[35] FFT-NLLS was based on a multicomponent cosine fit. Rhythm
214 significance was estimated by a relative amplitude error (RAE) that increases from 0 to 1 as the rhythm
215 approached statistical insignificance. These analyses were performed using R scripts developed and
216 run with R 3.6.3 (http://r-project.org/).[53]
217
218 **RNA-seq analysis.** Th*e L. aequinoctialis* Nd strain (6th generation of self-fertilization of the N35Kn04
219 strain)[33] was used for RNA-seq analysis. Plants were maintained under 15L9D conditions
220 (approximately 50 μmol m^{-2} s^{-1}, white LED T5LT20W, Beamtec, Japan) in an incubator (HCLP-880,
221 NK system, Japan) at 25 ± 1 °C. For the 14L10D and 12L12D experiments, the plants were divided
222 into 48 x 35-mm dishes (four colonies per dish) with 4 mL growth medium per dish. After one week

223 of photoperiodic treatment (14L10D or 12L12D), plants in each dish were collected every 2 h for 24
224 h (four replicates per sampling time). For the 9L15D experiment, plants were pre-cultured under
225 9L15D conditions for one week. Thereafter, these plants were divided into 24 x 35-mm dishes (six
226 colonies per dish) with 4 mL of growth medium per dish. After one week of photoperiodic treatment
227 (9L15D), plants in each dish were collected every 2 h for 24 h (two replicates at each sampling time).
228 The collected plants were wiped of moisture with paper, then immediately immersed in RNAlater
229 solution (Sigma Aldrich) at each time point and stored at -20 °C before RNA extraction. RNA-seq
230 library preparation was performed based on the BrAD-seq protocol, as follows.[54] Plants were
231 homogenized with a lysate buffer using a multi-bead shocker (MB755U, Yasui Kikai, Japan). mRNA
232 was extracted from the lysate using magnetic streptavidin beads (New England Biolabs) with a biotin-
233 20nt-20T oligo. The mRNA was subjected to heat fragmentation (94 °C for 1.5 min) and converted to
234 cDNA using RevertAid Reverse Transcriptase (Thermo Fisher) with a 3-prime priming adapter with
235 a random octamer sequence. The 5-prime adapter was then added to the cDNA and captured by the
236 terminus of the RNA-cDNA hybrid. Its incorporation into a complete library molecule was catalyzed
237 by DNA polymerase I (Thermo Fisher). The library was prepared using 16 (9L15D samples) or 18
238 (14L10D and 12L12D samples) PCR cycles with KAPA HiFi HS ReadyMix (Kapa Biosystems). The
239 fragment size was selected to range from 300 bp to 600 bp using Ampure magnetic beads (Beckman
240 Coulter). The quality of the library was checked using a bioanalyzer (Agilent). Paired-end 150 bp
241 sequencing was conducted using the HiSeq system (Illumina). The obtained sequences (total 554
242 million reads for the 120 samples) were filtered using Trimmomatic v0.39 with option "LEADING:24
243 TRAILING:24 SLIDINGWINDOW:30:20 AVGQUAL:20 MINLEN:100".[55] The filtered sequences
244 were assembled *de novo* into 322,899 contigs (isoforms of 186,102 genes) using Trinity v2.8.4.[56] The
245 183,102 contigs (isoforms of 84,206 genes) that were longer than 400 bp were used as a reference
246 sequence for mapping and read counting using RSEM v1.3.1 with bowtie2 v2.4.2.[57, 58] The mapped
247 reads were 3.46 ± 1.22 million reads / sample (mean ± SD).
248
249 **Detection of *FT* homologues**. *FT* homologues in the reference sequence (183,102 contigs) were
250 searched using tblastn 2.11.0+ [59] with a query for the OsHd3a amino acid sequence (UniProt-ID:
251 Q93WI9). The top five *FT* homologues were named as *LaFTh1-5* based on their position in the
252 maximum likelihood phylogenetic tree with their estimated amino acid sequences and AtFT (UniProt-
253 ID: Q9SXZ2), AtTSF (UniProt-ID: Q9S7R5), OsHd3a (UniProt-ID: Q93WI9), and OsRFT1(UniProt-
254 ID: Q8VWH2) (Fig. S5b). LaFTh2 and LaFTh4 have the same sequence as previously reported FT
255 homologues, LaFTL1 and LaFTL3, respectively.[60] A phylogenetic tree was constructed using the
256 online tool ClustalW (https://www.genome.jp/tools-bin/clustalw) using the PhyML algorithm.
257 Colored multiple amino acid sequence alignments were generated using the online tool Clustal Omega
258 (https://www.ebi.ac.uk/Tools/msa/clustalo/).

259

260 **qPCR analysis.** Eight to 12 colonies grown under 15L9D conditions were placed in a 35-mm dish
261 with 4 mL of growth medium and maintained under the same conditions for a day, after which they
262 were released to constant darkness at the end of 15 h of light and sampled every hour from 9 to 15 h
263 after the light-off. The collected plants were wiped of moisture with paper, then immediately immersed
264 in RNAlater solution (Sigma Aldrich) at each time point and stored at -20 °C before RNA extraction.
265 Total RNA was extracted using the NucleoSpin RNA Plant (MACHEREY-NAGEL GmbH & Co.) and
266 converted to cDNA using ReverTra Ace qPCR RT Master Mix (TOYOBO). qPCR was performed
267 using the StepOnePlus Real-Time PCR System (Applied Biosystems) with THUNDERBIRD SYBR
268 qPCR Mix (TOYOBO). An *ACT2* homologue in *de novo* assembled sequences was determined using
269 tblastn 2.11.0+ with a query of the OsACT2 amino acid sequence (UniProt-ID: A3C6D7) and used as
270 a reference gene for the delta-delta Ct method. Primers for qPCR analysis were designed according to
271 the *de novo* assembled sequences as follows: LaFTh1_fwd, 5'-
272 ACCCTACCCTTAGAGAATATCTGC-3'; LaFTh1_rev, 5'-TAGGTGCTGGGCCTTCATAG-3',
273 LaACT2_fwd, 5'-ACACAGTGCCCATCTATGAAGG-3'; LaACT2_rev, 5'-
274 AGTAGCCTCGTTCGGTTAGGATC-3'.
275

276 ***LaFTh1* overexpression in *Arabidopsis thaliana.*** To generate *LaFTh1* overexpressing transgenic
277 *Arabidopsis* plants, the coding region of *LaFTh1* was amplified from cDNA derived from *L.*
278 *aequinoctialis* Nd using the following primers: 5'-
279 CGCGGCCGCCACCATGACACCTCAGGATCCCTTGTG-3', and 5'-
280 CGGCGCGCCCTAGGTAAACCGCCTTCCACCAG-3'. The amplified PCR fragment was digested
281 with *Not*I and *Asc*I restriction enzymes and integrated into the pENTR-MCS cloning vector [pENTR-
282 D/TOPO vector (Invitrogen) containing the pBluescript II multi-cloning sites] using the conventional
283 linker ligation method. The sequence of *LaFTh1* CDS was transferred into the pK7WG2
284 overexpression binary vector,[61] which contained the *CaMV35S* promoter-driven expression cassette,
285 using Gateway LR clonase II (Invitrogen). This construct was introduced into *Arabidopsis* wild-type
286 plants Col-0 by the *Agrobacterium tumefaciens*-mediated floral dipping method.[62] Primary
287 transformants (T1) were selected on 1x Murashige and Skoog culture media containing 1% sucrose,
288 0.8% agar, and 25 μg mL^{-1} kanamycin sulfate. Seeds were sterilized using chlorine gas, stratified for
289 3 days at 4 °C, and then grown under short-day (10L14D) conditions to analyze the flowering
290 phenotype in parallel with the selection process. Seedlings developing relatively long primary and
291 lateral roots were regarded as kanamycin-resistant transgenic plants and transferred to a 1:1 mixture
292 of vermiculite and soil (Nihon Hiryo Co., Ltd.). Several independent lines ($N > 10$) were isolated for
293 further analysis of their morphological and flowering phenotypes. Most primary transformants could
294 not produce mature siliques or seeds; however, some transgenic plants produced T2 seeds. Flowering

295 phenotypes were also observed in the T2 generation.
296
297 **Statistics.** All boxplots in this manuscript display median lines, interquartile range boxes, and
298 min/max whiskers. Different letters indicate significant differences based on the pairwise Wilcoxon
299 test ($p < 0.05$). The pairwise Wilcoxon test was performed using the R built-in function
300 "pairwise.wilcox.test" with *P* value adjustment using the Holm method. In correlation analysis, the
301 Pearson's correlation coefficient and *P* value was calculated by the R-built-in function "cor.test".
302
303 **Data availability**
304 The RNA-seq raw sequences (PRJDB12719) and LaFTh1 CDS (LC662606) were deposited at DDBJ.
305
306 **Acknowledgements**
307 We thank N. Emura for her support in collecting duckweed strains, I. Shibano for her support in
308 maintaining duckweed strains, M. Honjo and M. Hirata for their support with RNA-seq experiments
309 in the Joint Usage for Ecological Research, Kyoto University, and S. Kubota for her efforts to establish
310 the Nd strain. This research was supported by the Japan Society for the Promotion of Science
311 KAKENHI [grant numbers JP16H06864 (T.M.), JP20K15861 (T.M.), JP20J00255 (T.M.),
312 JP20K06342 (S.I.), JP21H04977 (H.K), and 17KT0022 (T.O.)], Japan Science and Technology
313 Agency (JST) CREST（JPMJCR15O1, H.K.), JST ALCA (JPMJAL1108, T.O.), and JST SATREPS
314 (JPMJSA2004, T.M., S.I., T.O.).
315
316 **Author contributions**
317 T.M. and T.O. designed the study and wrote and revised the manuscript. T.M. performed the
318 experiments using *L. aequinoctialis* and all the analyses. S.I. performed the experiments using *A.*
319 *thaliana* and contributed to the particle bombardment experiments. H.K. contributed to RNA-seq
320 experiments and revised the manuscript. All authors have contributed to the text.
321
322 **Competing interests**
323 The authors declare no competing interests.
324

References

1. Barrett, R.D.H., and Schluter, D. (2008). Adaptation from standing genetic variation. Trends Ecol. Evol. *23*, 38–44.
2. Alonso-Blanco, C., Aarts, M.G.M., Bentsink, L., Keurentjes, J.J.B., Reymond, M., Vreugdenhil, D., and Koornneef, M. (2009). What has natural variation taught us about plant development, physiology, and adaptation? Plant Cell *21*, 1877–1896.
3. Matuszewski, S., Hermisson, J., and Kopp, M. (2015). Catch me if you can: adaptation from standing genetic variation to a moving phenotypic optimum. Genetics *200*, 1255–1274.
4. Boyle, E.A., Li, Y.I., and Pritchard, J.K. (2017). An Expanded view of complex traits: From polygenic to omnigenic. Cell *169*, 1177–1186.
5. Sella, G., and Barton, N.H. (2019). Thinking about the evolution of complex traits in the era of genome-wide association studies. Annu. Rev. Genomics Hum. Genet. *20*, 461–493.
6. Feiner, N., Brun-Usan, M., and Uller, T. (2021). Evolvability and evolutionary rescue. Evol. Dev. *23*, 308–319.
7. Helm, B., Visser, M.E., Schwartz, W., Kronfeld-Schor, N., Gerkema, M., Piersma, T., and Bloch, G. (2017). Two sides of a coin: ecological and chronobiological perspectives of timing in the wild. Philos. Trans. R. Soc. Lond. B. Biol. Sci. *372*, 20160246.
8. Michael, T.P., Park, S., Kim, T.S., Booth, J., Byer, A., Sun, Q., Chory, J., and Lee, K. (2007). Simple sequence repeats provide a substrate for phenotypic variation in the *Neurospora crassa* circadian clock. PloS One *2*, e795.
9. Brown, S.A., Kunz, D., Dumas, A., Westermark, P.O., Vanselow, K., Tilmann-Wahnschaffe, A., Herzel, H., and Kramer, A. (2008). Molecular insights into human daily behavior. Proc. Natl. Acad. Sci. U. S. A. *105*, 1602–1607.
10. Pivarciova, L., Vaneckova, H., Provaznik, J., Wu, B.C.H., Pivarci, M., Peckova, O., Bazalova, O., Cada, S., Kment, P., Kotwica-Rolinska, J., et al. (2016). Unexpected Geographic Variability of the Free Running Period in the Linden Bug *Pyrrhocoris apterus*. J. Biol. Rhythms *31*, 568–576.
11. Salmela, M.J., and Weinig, C. (2019). The fitness benefits of genetic variation in circadian clock regulation. Curr. Opin. Plant Biol. *49*, 86–93.
12. Hut, R.A., Paolucci, S., Dor, R., Kyriacou, C.P., and Daan, S. (2013). Latitudinal clines: An evolutionary view on biological rhythms. Proc. R. Soc. B Biol. Sci. *280*, 1–9.
13. Kubota, A., Shim, J.S., and Imaizumi, T. (2015). Natural variation in transcriptional rhythms modulates photoperiodic responses. Trends Plant Sci. *20*, 259–261.
14. Yukawa, I., and Takimoto, A. (1976). Flowering response of *Lemna paucicostata* in Japan. Bot. Mag. Tokyo *89*, 241–250.
15. Pittendrigh, C.S. (1960). Circadian rhythms and the circadian organization of living systems.

Cold Spring Harb. Symp. Quant. Biol. *25*, 159–184.

16. Saini, R., Jaskolski, M., and Davis, S.J. (2019). Circadian oscillator proteins across the kingdoms of life: Structural aspects. BMC Biol. *17*, 1–39.

17. Nagel, D.H., and Kay, S.A. (2012). Complexity in the wiring and regulation of plant circadian networks. Curr. Biol. *22*, R648-57.

18. Johnson, C.H., Elliott, J.A., and Foster, R. (2003). Entrainment of circadian programs. Chronobiol. Int. *20*, 741–774.

19. Schmal, C., Herzel, H., and Myung, J. (2020). Clocks in the wild: Entrainment to natural light. Front. Physiol. *11*, 1–12.

20. Aschoff, J., and Pohl, H. (1978). Phase relations between a circadian rhythm and its zeitgeber within the range of entrainment. Naturwissenschaften *65*, 80–84.

21. Lankinen, P. (1986). Geographical variation in circadian eclosion rhythm and photoperiodic adult diapause in *Drosophila littoralis*. J. Comp. Physiol. A *159*, 123–142.

22. Graf, A., Schlereth, A., Stitt, M., and Smith, A.M. (2010). Circadian control of carbohydrate availability for growth in *Arabidopsis* plants at night. Proc. Natl. Acad. Sci. U. S. A. *107*, 9458–9463.

23. Rémi, J., Merrow, M., and Roenneberg, T. (2010). A circadian surface of entrainment: varying T, τ, and photoperiod in *Neurospora crassa*. J. Biol. Rhythms *25*, 318–328.

24. Granada, A.E., Bordyugov, G., Kramer, A., and Herzel, H. (2013). Human chronotypes from a theoretical perspective. PloS One *8*, e59464.

25. Dominoni, D.M., Helm, B., Lehmann, M., Dowse, H.B., and Partecke, J. (2013). Clocks for the city: circadian differences between forest and city songbirds. Proceedings. Biol. Sci. *280*, 20130593.

26. Jiménez-Gómez, J.M., Lin, T., Srinivasan, A., Maloof, J.N., Müller, N.A., Ranjan, A., Ryngajllo, M., Sinha, N.R., Huang, S., West, D., et al. (2015). Domestication selected for deceleration of the circadian clock in cultivated tomato. Nat. Genet. *48*, 89–93.

27. Ray, P.M., and Alexander, W.E. (1966). Photoperiodic adaptation to latitude in *Xanthium strumarium*. Am. J. Bot. *53*, 806–816.

28. Imamura, S., Muramatsu, M., Kitajo, S.I., and Takimoto, A. (1966). Varietal difference in photoperiodic *Pharbitis nil*. Dot. Mag. Tokyo *79*, 714–721.

29. Katayama, T. (1977). Studies on the photoperiodism in the genus *Oryza*. Japan Agric. Res. Q. *11*, 12–17.

30. Natuhara, Y. (2013). Ecosystem services by paddy fields as substitutes of natural wetlands in Japan. Ecol. Eng. *56*, 97–106.

31. Fujita, G., Naoe, S., and Miyashita, T. (2015). Modernization of drainage systems decreases gray-faced buzzard occurrence by reducing frog densities in paddy-dominated landscapes. Landsc. Ecol. Eng. *11*, 189–198.

32. Landolt, E. (1986). Biosystematic investigation in the family of duckweeds ("*Lemnaceae*"). Vol. 2: the family of "*Lemnaceae*" – a monographic study. Volume 1 Veröffentlichungen des Geobotanischen Institutes der ETH, Stiftung Rubel, Zürich *78*, 142-146**.**

33. Muranaka, T., Okada, M., Yomo, J., Kubota, S., and Oyama, T. (2015). Characterisation of circadian rhythms of various duckweeds. Plant Biol. *17*, 66–74.

34. Nakamichi, N., Ito, S., Oyama, T., Yamashino, T., Kondo, T., and Mizuno, T. (2004). Characterization of plant circadian rhythms by employing *Arabidopsis* cultured cells with bioluminescence reporters. Plant Cell Physiol. *45*, 57–67.

35. Zielinski, T., Moore, A.M., Troup, E., Halliday, K.J., and Millar, A.J. (2014). Strengths and limitations of period estimation methods for circadian data. PloS One *9*, e96462.

36. Hayama, R., Agashe, B., Luley, E., King, R., and Coupland, G. (2007). A circadian rhythm set by dusk determines the expression of FT homologs and the short-day photoperiodic flowering response in Pharbitis. Plant Cell *19*, 2988–3000.

37. Hut, R.A., and Beersma, D.G.M. (2011). Evolution of time-keeping mechanisms: Early emergence and adaptation to photoperiod. Philos. Trans. R. Soc. B Biol. Sci. *366*, 2141–2154.

38. Katayama, N., Baba, Y.G., Kusumoto, Y., and Tanaka, K. (2015). A review of post-war changes in rice farming and biodiversity in Japan. Agric. Syst. *132*, 73–84.

39. Michael, T.P., Salomé, P.A., Yu, H.J., Spencer, T.R., Sharp, E.L., McPeek, M.A., Alonso, J.M., Ecker, J.R., and McClung, C.R. (2003). Enhanced fitness conferred by naturally occurring variation in the circadian clock. Science. *302*, 1049–1053.

40. Rieseberg, L.H., Widmer, A., Arntz, A.M., Burke, J.M., Carr, D.E., Abbott, R.J., and Meagher, T.R. (2003). The genetic architecture necessary for transgressive segregation is common in both natural and domesticated populations. Philos. Trans. R. Soc. B Biol. Sci. *358*, 1141–1147.

41. Hamann, E., Pauli, C.S., Joly-Lopez, Z., Groen, S.C., Rest, J.S., Kane, N.C., Purugganan, M.D., and Franks, S.J. (2021). Rapid evolutionary changes in gene expression in response to climate fluctuations. Mol. Ecol. *30*, 193–206.

42. Beppu, T., and Takimoto, A. (1981). Geographical distribution and cytological variation of *Lemna paucicostata* Hegelm. In Japan. Bot. Mag. Tokyo *94*, 11–20.

43. Wang, W., Kerstetter, R.A., and Michael, T.P. (2011). Evolution of genome size in duckweeds (*Lemnaceae*). J. Bot. *2011*, 1–9.

44. Sémon, M., and Wolfe, K.H. (2007). Consequences of genome duplication. Curr. Opin. Genet. Dev. *17*, 505–512.

45. Selmecki, A.M., Maruvka, Y.E., Richmond, P.A., Guillet, M., Shoresh, N., Sorenson, A.L., De, S., Kishony, R., Michor, F., Dowell, R., et al. (2015). Polyploidy can drive rapid adaptation in yeast. Nature *519*, 349–351.

46. Greenham, K., and McClung, C.R. (2015). Integrating circadian dynamics with

433 physiological processes in plants. Nat. Rev. Genet. *16*, 598–610.
434 47. Urbanová, V., Bazalová, O., Vaněčková, H., and Dolezel, D. (2016). Photoperiod regulates
435 growth of male accessory glands through juvenile hormone signaling in the linden bug, *Pyrrhocoris*
436 *apterus*. Insect Biochem. Mol. Biol. *70*, 184–190.
437 48. Dixon, L.E., Hodge, S.K., van Ooijen, G., Troein, C., Akman, O.E., and Millar, A.J. (2014).
438 Light and circadian regulation of clock components aids flexible responses to environmental signals.
439 New Phytol. *203*, 568–577.
440 49. Nagel, D.H., and Kay, S.A. (2012). Complexity in the wiring and regulation of plant
441 circadian networks. Curr. Biol. *22*, R648-57.
442 50. Sun, L., Dong, A., Griffin, C., and Wu, R. (2021). Statistical mechanics of clock gene
443 networks underlying circadian rhythms. Appl. Phys. Rev. *8*, 021313.
444 51. Schneider, C.A., Rasband, W.S., and Eliceiri, K.W. (2012). NIH Image to ImageJ:
445 25 years of image analysis. Nat. Methods *9*, 671–675.
446 52. Muranaka, T., and Oyama, T. (2016). Heterogeneity of cellular circadian clocks in intact
447 plants and its correction under light-dark cycles. Sci. Adv. *2*, e1600500.
448 53. Ihaka, R., and Gentleman, R. (1996). R: A language for data analysis and graphics.
449 J. Comput. Graph. Stat. *5*, 299–314.
450 54. Townsley, B.T., Covington, M.F., Ichihashi, Y., Zumstein, K., and Sinha, N.R. (2015).
451 BrAD-seq: Breath Adapter Directional sequencing: A streamlined, ultra-simple and fast library
452 preparation protocol for strand specific mRNA library construction. Front. Plant Sci. *6*, 1–11.
453 55. Bolger, A.M., Lohse, M., and Usadel, B. (2014). Trimmomatic: A flexible trimmer
454 for Illumina sequence data. Bioinformatics *30*, 2114–2120.
455 56. Grabherr, M.G., Haas, B.J., Yassour, M., Levin, J.Z., Thompson, D.A., Amit, I.,
456 Adiconis, X., Fan, L., Raychowdhury, R., Zeng, Q., et al. (2011). Full-length transcriptome
457 assembly from RNA-Seq data without a reference genome. Nat. Biotechnol. *29*, 644–652.
458 57. Li, B., and Dewey, C.N. (2011). RSEM: accurate transcript quantification from
459 RNA-Seq data with or without a reference genome. BMC Bioinformatics *12*, 323.
460 58. Langmead, B., and Salzberg, S.L. (2012). Fast gapped-read alignment with Bowtie
461 2. Nat. Methods *9*, 357–359.
462 59. Altschul, S.F., Gish, W., Miller, W., Myers, E.W., and Lipman, D.J. (1990). Basic
463 local alignment search tool. J. Mol. Biol. *215*, 403–410.
464 60. Yoshida, A., Taoka, K., Hosaka, A., Tanaka, K., Kobayashi, H., Muranaka, T., Toyooka, K.,
465 Oyama, T., and Tsuji, H. (2021). Characterization of frond and flower development and identification
466 of FT and FD genes from duckweed *Lemna aequinoctialis* Nd. Front. Plant Sci. *12*, 697206.
467 61. Karimi, M., Inzé, D., and Depicker, A. (2002). GATEWAY vectors for *Agrobacterium*-
468 mediated plant.pdf. Trends Plant Sci. *7*, 193–195.

469 62. Zhang, X., Henriques, R., Lin, S.S., Niu, Q.W., and Chua, N.H. (2006). *Agrobacterium-*
470 mediated transformation of *Arabidopsis thaliana* using the floral dip method. Nat. Protoc. *1*, 641–646.

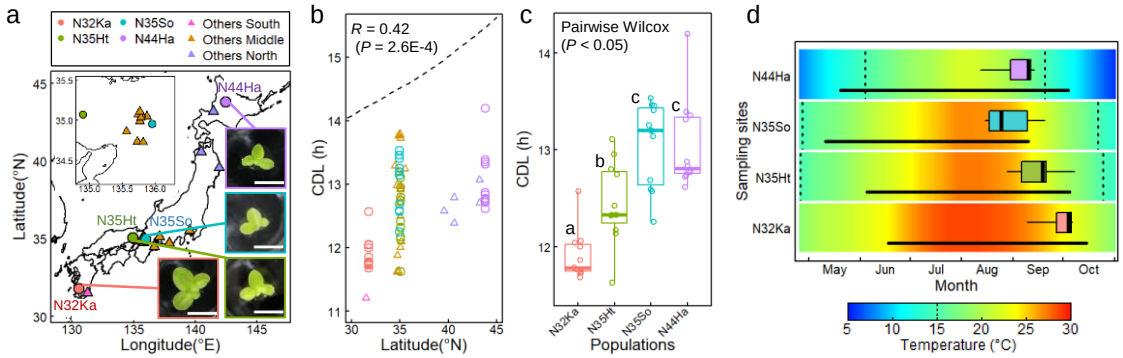

Fig. 1 Local adaptation of critical day-length (CDL) in *Lemna aequinoctialis* strains isolated in Japan. A, The locations from which 11–12 strains (circles) and 1–3 strains (triangles) were isolated. The same colors and symbols apply to other panels. Examples of the strains in the four populations are shown. Scale bars: 5 mm. **b**, Latitudinal cline of CDL. The Pearson's correlation coefficient and *P* value are shown. Dashed line represents day-length of summer solstice. **C,** CDL variation among the four populations. Boxplots with points representing individual strains are shown. **D,** Timing of CDLs in the year at four sampling sites. The dates for CDLs shown in panel c are represented as a box plot at each site. Black horizontal lines represent the flooding period. The background colors represent 30-year (1990–2019) mean of daily temperature. Vertical dotted lines represent 15 °C.

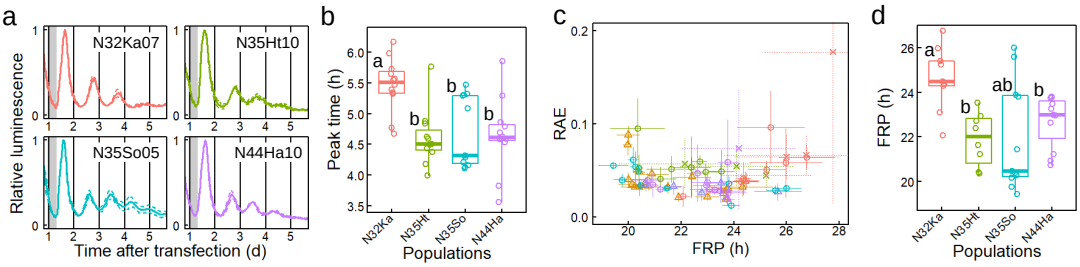

Fig. 2 Natural variation of circadian rhythms in *Lemna aequinoctialis* strains. A, Examples of luminescence rhythms of *AtCCA1::LUC*. Solid and dashed lines represent mean and ± SD of three replications, respectively. Gray boxes indicate dark period. The strain name is indicated in each plot. **B,** Variation of the timing of the first peak in constant light (LL) among the four populations. Boxplots with points for individual strains are shown. **C**, Relative amplitude error (RAE) of each strain plotted against its free running period (FRP). Mean values of three replications are shown. Error bars = SD. The crosses represent seven strains that showed unstable rhythms (SD of FRP > 1.5 h, Fig. S4). Population names are represented in the graph legend. **D,** Variation of the free-running period (FRP) in LL among the four populations. Boxplots with points for individual strains are shown. Seven strains with unstable rhythms (SD of FRP > 1.5 h) were excluded from the plot.

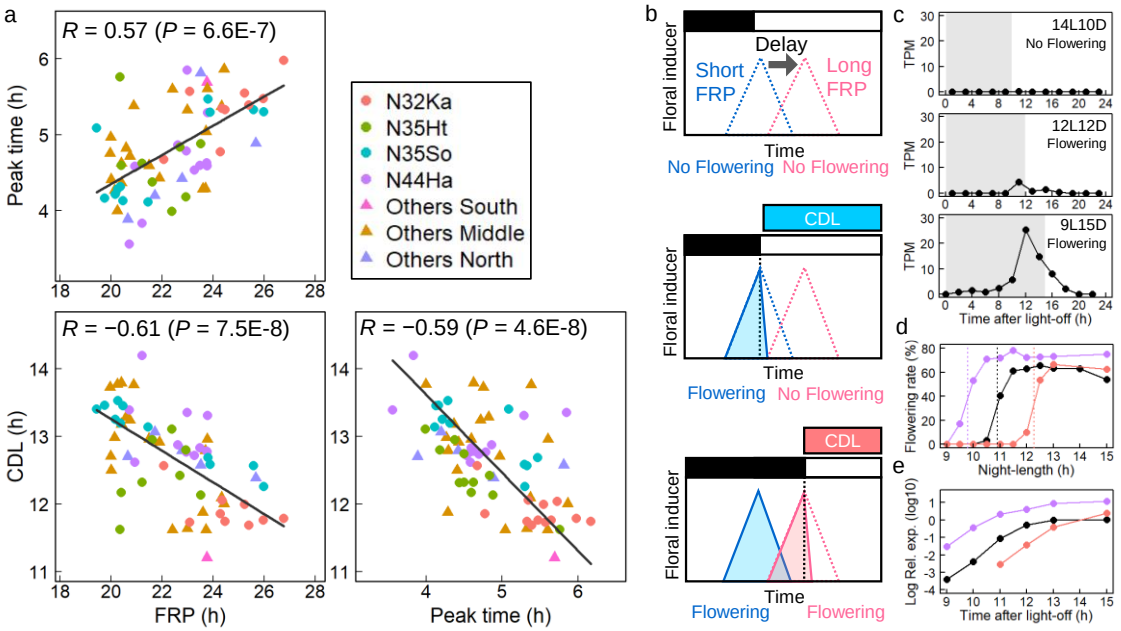

Fig. 3 Chronotype effect on photoperiodic flowering. A, The correlations between FRP, peak time, and CDL of *L. aequinoctialis* strains. The Pearson's correlation coefficient and *P* value are shown in each graph. Black lines represent Deming regression lines. Plots of seven strains with unstable rhythms (SD of FRP > 1.5 h) are excluded from graphs that include FRP. **B,** The hypothetical mechanism for the negative correlation between FRP and CDL. The activation of the floral inducer is assumed to be gated by the circadian clock and permitted in the dark. The dotted lines and filled triangles schematically represent gate timing and activity of a floral inducer, respectively. The blue and red colors correspond to strains with a short and long FRP, respectively. **C,** A photoperiodic response of the *LaFTh1* expression. Means of four or two RNA-seq experiments are plotted. Gray box indicates a dark period. **D,** Photoperiodic responses of flowering for three strains (purple, N44Ha08; black, Nd; red, N32Ka06). The flowering rates are plotted against the night length of each photoperiod. The critical night length (24 – CDL) of each strain is shown as dashed line. **E,** *LaFTh1* induction in the three strains during constant dark following 15L9D. The mRNA accumulation quantified by qPCR is plotted. The mRNA expression in N32Ka06 at 9 and 10 h were undetected. Colors are the same as in panel d.

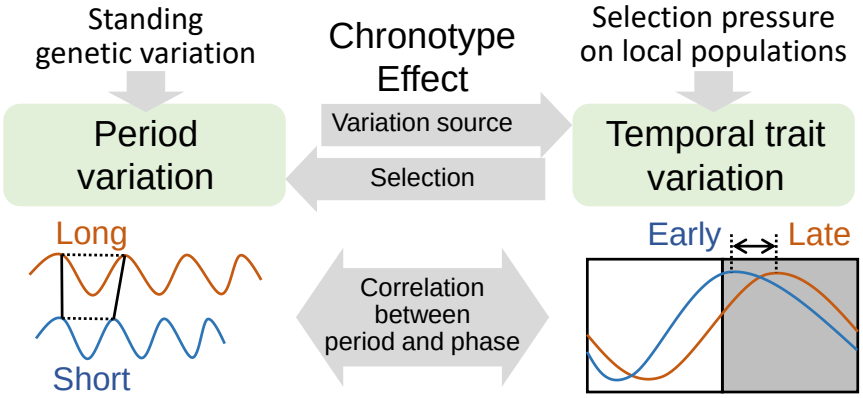

Fig. 4 The chronotype effect on local adaptation of clock-dependent temporal traits. FRP variation functions as a resource for the variation of temporal traits in the process of local adaptation. Genetic variations in many quantitative loci for FRP are selected based on their phenotypic effect on temporal traits under day-night conditions. In *L. aequinoctialis*, the selection pressure for early-flowering phenotype appeared to select a short-FRP genotype related to its early induction timing of a florigen gene.

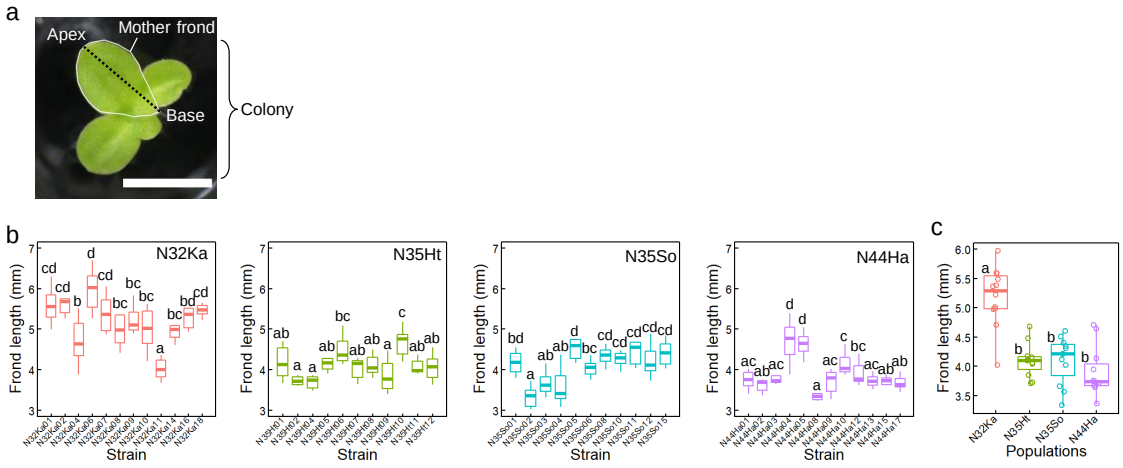

Figure S1. Intra- and inter-population variation of frond length in *L. aequinoctialis* strains. a, Definition of a frond length. The length of the mother frond (from base to apex, dotted black line) of eight colonies were measured for each strain of four populations (N32Ka, N35Ht, N35So, and N44Ha). Scale bar indicates 5 mm. **b,** Intra-population variation of frond length of the four populations are shown as boxplots. Different letters indicate significant differences based on Tukey's HSD test ($P < 0.05$). **c,** Inter-population variation of frond length among the four populations. Different letters indicate significant differences based on pairwise Wilcoxon test ($P < 0.05$). Boxplots display a median line, interquartile range boxes, min/max whiskers.

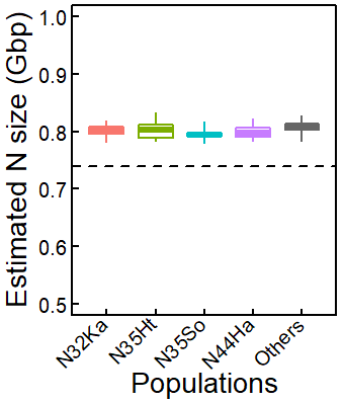

535

536

537 **Figure S2. Similar genome sizes among 72 strains in different populations**. Box plot displays a
538 median line, interquartile range boxes, min/max whiskers of estimated genome sizes of the strains in
539 a population (N32Ka, N35Ht, N35So, and N44Ha). "Others" includes 16 populations, which are
540 indicated by triangles in Fig. 1a. The genome size of a strain was estimated by flow cytometer. A
541 dashed line represents the estimated genome size of *L. aequinoctialis* 6746 strain isolated in California,
542 USA. No significant difference was detected based on pairwise Wilcoxon test.

543

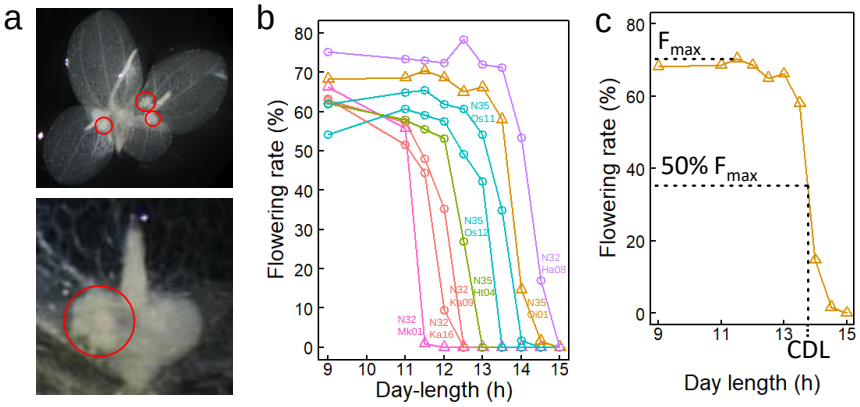

Figure S3. Photoperiodic response of flowering. a, A colony with floral buds (top). Colony of N35Oi03 strain bleached by EtOH after one week of short-day (9L15D) treatment and imaged from the underside. Close-up underside view around the meristematic tissue. Red circles indicate floral buds. **b,** Continuous variation of photoperiodic response on flowering. Flowering rate after one week of photoperiodic treatment is plotted against treated day-length. Eight strains in six populations are shown. **c**, Definition of critical day length (CDL). Flowering rates under nine photoperiod conditions were measured. CDL was determined as the day-length where 50% of the maximum flowering rate (Fmax) is expected. See Methods for more detail.

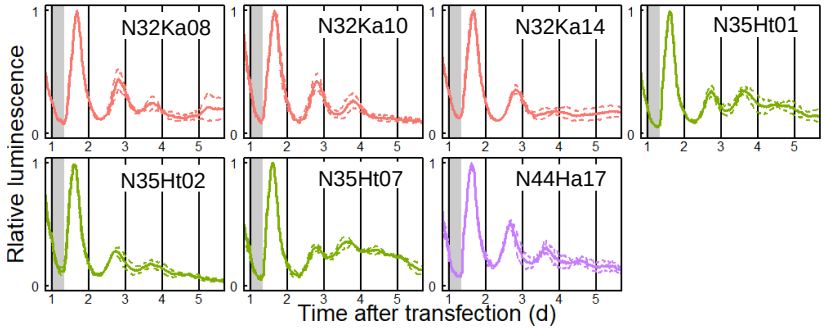

Figure S4. Luminescence rhythms of the seven strains excluded from the analysis. Luminescence intensity at each time point was normalized by the maximum intensity (first peak value). Solid and dashed lines represent mean and SD of three replications, respectively. Same populations are represented by the same colors.

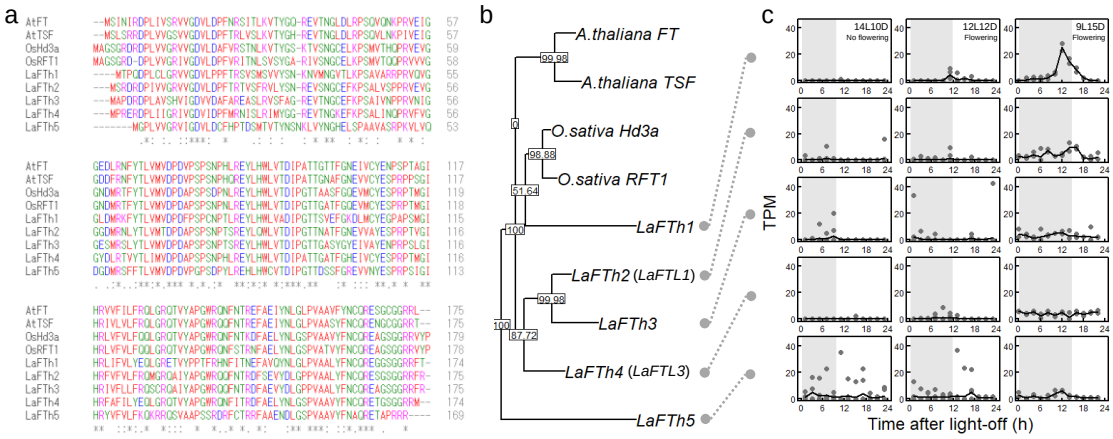

Figure S5. FT homologues of *L. aequinoctialis* Nd strain. **a,** Multiple amino acid sequence alignment of the five FT homologues (LaFTh1-5) with the florigen of *Arabidopsis thaliana* (AtFT and AtTSF) and *Oryza sativa* (OsHd3a and OsRFT1). Colors represent physicochemical properties of residues. **b,** Maximum likelihood phylogenetic tree constructed with PhyML algorithm using full-length amino acid sequences. **c,** The expression patterns of five FT homologues (LaFTh1 to LaFTh5 from top to bottom) under three photoperiods (14L10D, 12L12D, 9L15D from right to left). The transcripts per kilobase million (TPM) values are plotted. Two (9L15D) or four (12L12D and 14L10D) experiments were performed for each photoperiodic condition. Black lines represent the mean values at each time point. Gray boxes indicate dark period.

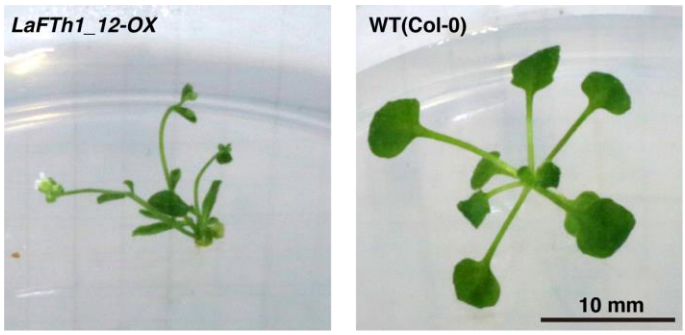

Figure S6. Early flowering phenotype of *A. thaliana* carrying an *LaFTh1* overexpression construct. Plants of an *LaFTh1* overexpression line (T2 generation) (left) and Col-0 wild type (right) on an agar plate at 22 °C and 24 days (10L14D) after sowing.

#	Population name	Symbol in Figs	Sampling site	Water system	Latitude	Longitude	Number of isolated strains
1	N44Ha	N44Ha	Asahikawa, Hokkaido	Paddy field	43.80468	142.45088	12
2	N43Hi	Others North	Ishikari, Hokkaido	Paddy field	43.1943	141.45465	2
3	N41Ac	Others North	Hirosaki castle, Aomori	Castle moat	40.60337	140.46717	2
4	N40Im	Others North	Miyako, Iwate	Paddy field	39.56776	141.93836	1
5	N36Ky	Others Middle	Yokohama, Kanagawa	Paddy field	35.52783	139.52045	1
6	N35At	Others Middle	Togo, Aichi	Paddy field	35.11062	137.083	1
7	N35Ki	Others Middle	Iwakura, Kyoto	Paddy field	35.07706	135.78781	2
8	N35Ht	N35Ht	Taka, Hyogo	Paddy field	35.07304	134.90231	11
9	N35Kk	Others Middle	Kyoto, Kyoto	Paddy field	35.07206	135.74302	1
10	N35Sb	Others Middle	Biwako, Shiga	Lake	35.04908	135.87446	3
11	N35Kn	Others Middle	Nougaku, Kyoto	Paddy field	35.03259	135.7836	3
12	N35Kr	Others Middle	Kamogawa river, Kyoto	Rivier	34.9896	135.76769	1
13	N35So	N35So	Otsu, Shiga	Paddy field	34.95615	135.95493	11
14	N35Oi	Others Middle	Ibaraki, Osaka	Paddy field	34.85884	135.56461	3
15	N35Nn	Others Middle	NAIST, Nara	Paddy field	34.7317	135.73142	2
16	N35Nk	Others Middle	Kizugawa, Nara	Paddy field	34.7242	135.8158	1
17	N35Si	Others Middle	Iwata, Shizuoka	Paddy field	34.72128	137.89284	1
18	N34Mi	Others Middle	Ise, Mie	Paddy field	34.49805	136.67711	1
19	N32Ka	N32Ka	Aira, Kagoshima	Paddy field	31.77734	130.56278	12
20	N32Mk	Others South	Kushimoto, Miyazaki	Paddy field	31.51068	131.25419	1

Table S1. Summary of twenty sampling sites.